JOURNAL OF AIRCRAFT
Vol. 44, No. 2, March–April 2007

Engineering Notes

ENGINEERING NOTES are short manuscripts describing new developments or important results of a preliminary nature. These Notes should not exceed 2500 words (where a figure or table counts as 200 words). Following informal review by the Editors, they may be published within a few months of the date of receipt. Style requirements are the same as for regular contributions (see inside back cover).

Aerodynamic Characterization of Grid Fins at Subsonic Speeds

P. Theerthamalai*
Defence Research and Development Laboratory, Hyderabad 500 058, India

DOI: 10.2514/1.27653

Nomenclature

C_A = axial force coefficient
C_m = pitching moment coefficient
C_N = normal force coefficient
M = Mach number
$\boldsymbol{n}$ = normal vector to the web, $[\boldsymbol{n}_x \quad \boldsymbol{n}_y \quad \boldsymbol{n}_z]$
$\boldsymbol{u}$ = local velocity vector, $[\boldsymbol{u}_x \quad \boldsymbol{u}_y \quad \boldsymbol{u}_z]$
V_∞ = freestream velocity
α = freestream angle of attack
δ = fin deflection

I. Introduction

A GRID fin or lattice fin is a nonconventional aerodynamic lifting and control surface consisting of an outer frame having internal grid framework of small chord length. The main advantage of the grid fin is low hinge moment due to low chord length and hence the size of the control actuator is small. The other advantages of the grid fin are 1) efficient packaging and suitability for tube launching, 2) good lift characteristics at supersonic speeds, 3) very high stall angle of attack, and 4) high strength to weight ratio. The main drawbacks of grid fin are 1) high drag, 2) less efficient at transonic speeds, and 3) complex structure.

Prediction methods have been reported for aerodynamic characterization of grid fins. The vortex lattice method has been used for subsonic flows for linear characteristics and empirical relation using experimental data for nonlinearity [1,2]. Empirical relation based on experimental data has been used for transonic speeds [3]. Evvard's theory has been used for supersonic flows for linear characteristics and empirical relation using experimental data for nonlinearity [4]. Shock expansion theory with separated body vortex has also been used for the prediction of supersonic aerodynamic characteristics [5].

Computational methods have been in use for analyzing the flow features of grid fins [6,7] and comparison of planar and grid fins [8]. Effect of orientation of the individual grid fin with respect to flow direction has also been brought out in the computational studies. The effect of grid-fin thickness, frontal shape, and ramp fairing upstream of the blunt base upon which the grid-fin assembly mounted have been investigated [9]. Many wind tunnel test studies have been reported to study the effect of Mach number, angle of attack, roll angles, grid configuration, grid density, etc. [10–12].

Even though grid fins are highly efficient at supersonic Mach numbers, grid fins are used at subsonic Mach numbers in some air-launched munitions due to its easy packaging and deploying capability. The objective of the present paper is to develop a methodology to predict the aerodynamic characteristics of grid fin without and with body at subsonic Mach numbers.

II. Prediction Methodology

The prediction method is based on vortex lattice theory for linear aerodynamics and empirical relation based on observation of experimental data. Body upwash is modeled using doublet in the crossflow. To predict the characteristics of the leeward fins accurately, body separated vortices are modeled using empirical relation. Control surface deflection and roll orientation effects are modeled taking effective angle of attack for each web of the grid fin.

The coordinate system is located at the nose of the body with right-hand notation. The x axis is along the body, y axis is along the right side viewed from the rear side, and the z axis is upward. The grid-fin geometry is divided into its constituent webs and each web is divided into a number of lifting panels. Fin deflection is modeled by rotation of webs about the hinge line. Roll orientation is modeled by rotation about the x axis. Knowing the corner points of each panel, the normal to the panel can be evaluated.

A. Vortex Lattice Network

The vortex lattice network is similar to those used in [1–3] and is presented in brief for completeness. The grid fin is divided into its constituent webs and each web is divided into small panels. Each panel is defined by four corner points and a horseshoe vortex is placed on each panel. The horseshoe vortex contains a bound vortex segment and two side segments along the panel edges up to the trailing edge of the web and extending to infinity in $\alpha/2$ direction. The bound vortex is placed at one-fourth chord location and a control point is placed at midpoint of three-fourths chord location. To determine the force on each web, the strength of each vortex has to be evaluated. The strength of the vortices is obtained by applying zero normal velocity condition at the control points of each panel. The normal velocity at the control point is composed of four components, the freestream velocity, the body upwash, the separated body vortex component, and the velocity from the grid-fin vortex network. The velocity induced by fin vortices is determined using the Biot–Savart equation. The velocity due to the presence of body is evaluated using upwash theory. The carryover force on the body due to fin is evaluated using a method of images as explained in [5].

B. Velocity Due to Separated Body Vortex

According to upwash theory, the leeward side-fin angle of attack and normal force will be almost the same as that of the windward side. But, the experimental results [12] show that the leeward fin forces are much smaller compared with the windward fin forces. The reason for the difference in forces between the leeward and windward fins is due to the body vortex separation on the leeward side and its influence on the leeward side fin. The leeward side vortices are modeled using empirical relation [13], which gives the location and

Received 6 September 2006; revision received 29 November 2006; accepted for publication 1 December 2006.

*Scientist, Directorate of Aerodynamics.

the strength of the vortex as a function of the distance from the point of vortex separation. The point of vortex separation is also given in [13] as a function of angle of attack and nose shape. Two symmetric vortices with two image vortices are used for the effect of the body vortices. Vortex core model has been used to maintain realistic induced velocities near the core [14].

C. Nonlinearity at Angles of Attack

The vortex lattice solution is based on linear potential flow theory and hence is applicable for low angles of attack of 5–8 deg. This linear theory is inadequate for grid fin, which is used on missiles with high maneuverability and hence high angles of attack. The formulation presented in [2] is

$$C_N = C_{N\alpha}(\alpha + \delta)/\lfloor 1 + K_1(\alpha + \delta)^2 \rfloor + C_{N\text{wash}} \tag{1}$$

In the preceding formulation, the value of K_1 is obtained by assuming the fin frontal area appears as a solid block at angle of attack of $\pi/4$ (45 deg). The second term in Eq. (1) is due to nonlinearity in the body upwash.

The present formulation is similar to [2] without the upwash term. The separated body vortex effect included in the present method models the nonlinear behavior of the leeward side fins. Hence, the nonlinear upwash term is dropped and the present formulation is

$$C_N = C_{N\alpha}\alpha_{\text{eff}}/(1 + K_1\alpha_{\text{eff}}^2) \tag{2}$$

where α_{eff} is the effective angle of attack, which includes freestream angle of attack, body upwash, separated body vortex effect, roll effect, and control surface deflection, and is given by

$$\alpha_{\text{eff}} = \sin^{-1}\left(\frac{\boldsymbol{u} \circ \boldsymbol{n}}{V_\infty}\right) = \sin^{-1}\left(\frac{\boldsymbol{u}_x\boldsymbol{n}_x + \boldsymbol{u}_y\boldsymbol{n}_y + \boldsymbol{u}_z\boldsymbol{n}_z}{V_\infty}\right) \tag{3}$$

The value of K_1 is determined by assuming the value of $\alpha_{\max}$. In [2], $\alpha_{\max}$ is assumed to be $\pi/4$. Different values of $\alpha_{\max}$ have been considered and found $\pi/6$ gives accurate results for most of the configurations. Hence, $\alpha_{\max}$ value of $\pi/6$ is used in the present formulation and the value of K_1 is determined as $1/\alpha_{\max}^2$.

The external flow sides behavior is similar to planar fins, which stalls around 15 deg, hence $\alpha_{\max}$ for external webs are taken as $\pi/12$. In the present method, the nonlinearity is addressed in web level, whereas in [1–3] the nonlinearity is applied to fin as a whole.

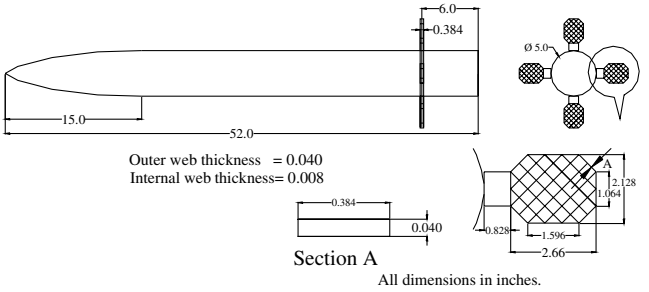

Fig. 1 Configuration G1.

D. Effect of Mach Number

The normal force over planar fins increases with Mach number in subsonic flows and Prandtl–Glauert compressibility correction is used for Mach number effect. In [1–3], a compressible form of the Biot–Savart equation is used. However, the experimental data [3] show that the normal force coefficient of grid fins reduces slightly with Mach number. Hence, in the present method, an incompressible form of vortex lattice solution is used and for Mach number effect the following relation is used.

$$(C_N)_{\text{at}M} = (C_N)_{\text{at}M=0} \times (1 - M^2)^{1/6} \tag{4}$$

E. Fin Axial Force Coefficient

Fin axial force is estimated at zero angle of attack and assumed to be the same at angles of attack. The general shape of the grid-fin cross section is constant thickness flat plate. Therefore, the axial force is composed of skin friction drag, leading-edge drag, and trailing-edge base drag. The skin friction drag is evaluated using equivalent flat plate skin friction coefficient, and leading-edge drag and base drag are evaluated using empirical relation [15].

III. Validation with Experimental Data

The prediction method has been applied to various grid-fin configurations and the results obtained are compared with available experimental data. The experimental data for validation have been taken from [2,11,12]. The experiments were conducted with different grid-fin designs mounted on a 10.4 caliber body of revolution with a three-caliber tangent ogive nose (Fig. 1). The

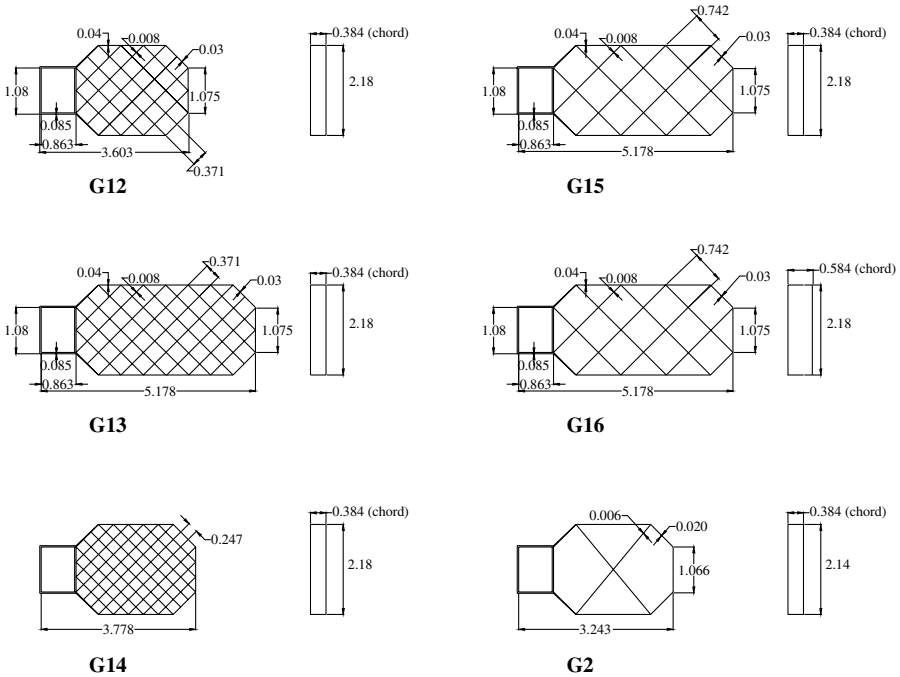

Fig. 2 Different grid-fin configurations used for validation.

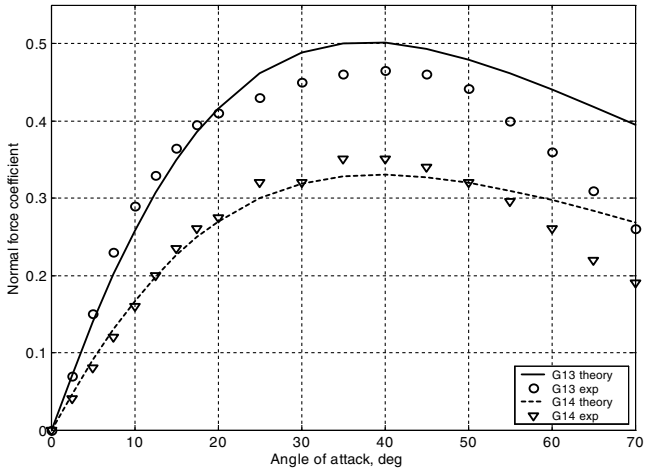

Fig. 3 Comparison of predicted normal force with experiment for isolated grid fins, $M = 0.35$.

various grid fins used for testing are shown in Fig. 2. The grid fins were mounted on the body at 1.2 calibers ahead of base. The comparison of predicted aerodynamic characteristics with experiment on isolated grid fin, grid fin on body, and with deflected grid fin is presented. All the forces and moments are based on body cross-sectional area and body diameter, even for the isolated fin coefficients. The moment reference point is main balance center, which is at 5.2 calibers from nose tip.

A. Fin Alone Configurations

The wind tunnel test data for validation of grid fin alone configuration are taken from [12]. The test data on isolated grid fins are available for configurations G13 and G14 at Mach number 0.35. The quoted accuracy of the fin balance used for the testing is 1.5% of the rated loads, which results in an accuracy of 8.9 N for normal force. The reported repeatability accuracy is 0.1% of the rated loads. The comparison of predicted normal force with experimental data for the two configurations is shown in Fig. 3. Even though the present formulation is not valid for very high angle of attack, the predicted normal force coefficient is presented up to 70 deg of angle of attack. The comparison shows that the predicted normal force compares well with experimental data up to an angle of attack of 50 deg and the deviation of prediction from experiment is within 12%.

B. Grid Fin Mounted on Body Configurations

Six different configurations are used for the validation of grid fin with body. The grid-fin configurations used for the validation are

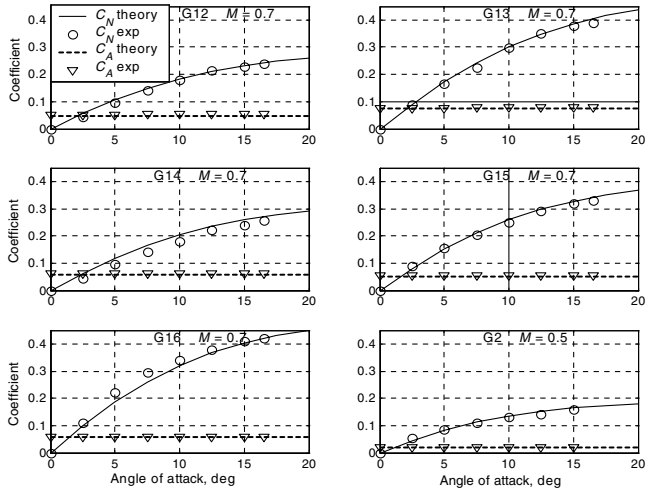

Fig. 4 Comparison of predicted normal and axial force with experiment for horizontal fins.

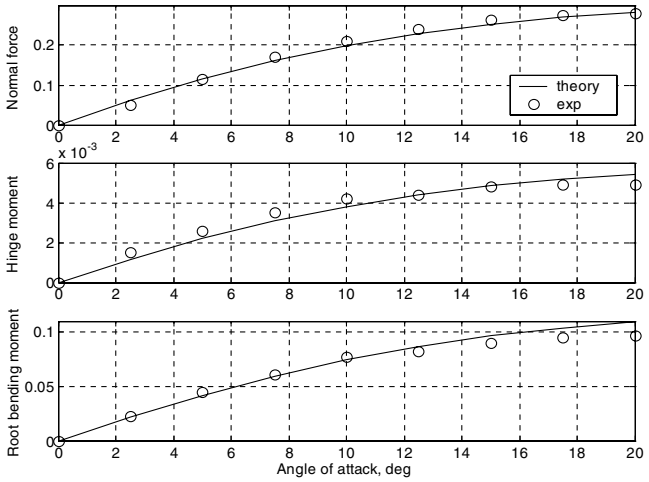

Fig. 5 Normal force, hinge moment, and bending moment for configuration G1, $M = 0.7$.

shown in Fig. 2 and the test data are taken from [12]. The test Mach number is 0.7 for all the configurations except for configuration G2, for which the test Mach number is 0.5. The test Reynolds number is not given in [12] and the value is taken as $Re = 2.36 \times 10^6$ based on body diameter from similar tests [11]. The balance used for fin-alone tests was used for these tests and hence the tests data accuracy is same as fin-alone tests. The predicted normal force and axial force coefficient of the horizontal fin is shown in Fig. 4 along with experimental data. The predicted values are in good agreement with the experimental data for all the configurations. The deviation of predicted normal force coefficient with experiment is less than 15%. The comparison of predicted axial force coefficient with experiment is also good and the maximum deviation is within 10%.

C. Hinge Moment Characteristics

Hinge moment and root bending moment characteristics have been predicted for the configuration G1. The predicted normal force, hinge moment about mid chord, and bending moment about root chord are compared with experimental data [11] in Fig. 5. The prediction compares well with experiment for all the coefficients and the maximum deviation is around 12%.

D. Characteristics with Control Surface Deflection

Aerodynamic characteristics of body with deflected grid-fin configuration have been evaluated for configuration G1. The test Mach number is 0.5 and $Re = 22.7 \times 10^6$ based on model diameter. The quoted accuracy of the fin balance is 2.5% of the rated loads,

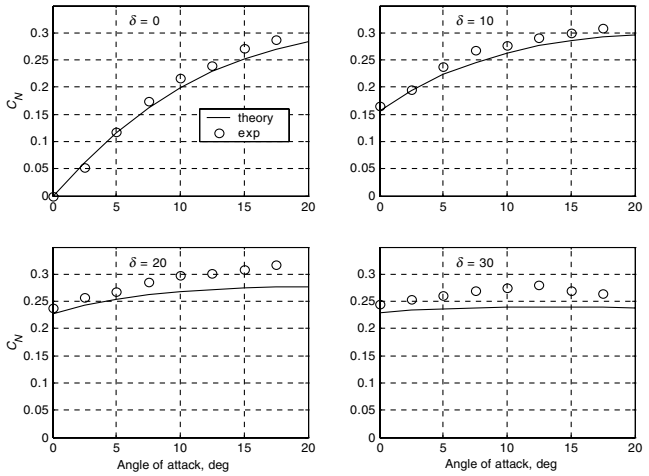

Fig. 6 Horizontal fin normal force for different fin deflections for configuration G1, $M = 0.5$.

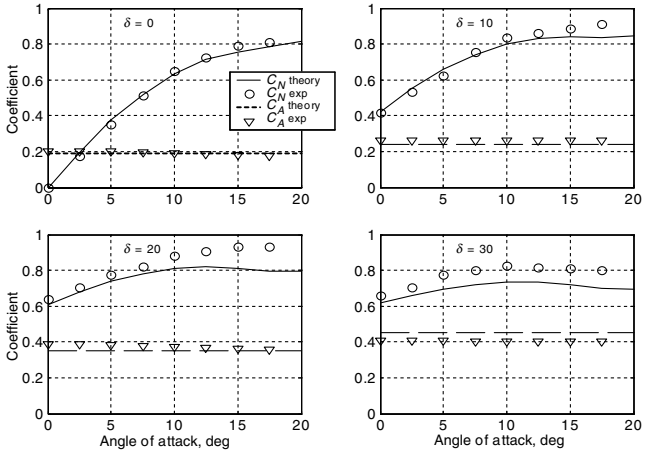

Fig. 7 Normal and axial force for cruciform fin body combination, configuration G1, $M = 0.5$.

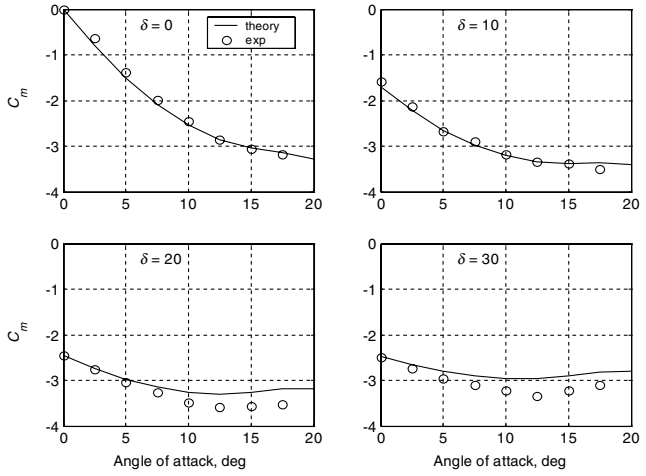

Fig. 8 Pitching moment coefficient for cruciform fin body combination, configuration G1, $M = 0.5$.

which is ± 22 N for the normal force and ± 0.56 N · m for the pitching moment. The reported repeatability accuracy is within 0.1% of the rated loads. The horizontal fin normal force with angle of attack for control surface deflection of 0, 10, 20, and 30 deg is presented in Fig. 6 along with the experimental data [2]. The comparison is good for all control surface deflection cases and the maximum deviation is within 12%. The comparison of normal force and axial force for combination of all the four cruciform fins with body carryover load is shown in Fig. 7. The pitching moment about balance center (5.2 calibers from nose tip) is shown in Fig. 8. The comparison shows that the theory predicts the characteristics very well for all the cases.

IV. Conclusions

A prediction method for the estimation of aerodynamic characteristics of grid-fin configurations at subsonic speeds is presented. The method is based on a vortex lattice method for linear component and empirical relation based on general trends of the available experimental data. Effect of body is modeled by using doublet in the crossflow plane. The separated body vortices are modeled using empirical data on separation point, separated vortex location, and strength. The predicted characteristics are compared with available experimental data for different configurations and the comparison shows:

1) The method predicts normal force, axial force, and pitching moment of individual fins and cruciform combination well. The deviation of prediction with experiment is within 15%.

2) The prediction of the normal force on isolated fin is good up to an angle of attack of 50 deg.

3) Prediction of fin deflection characteristics is also good even for higher fin deflection of 30 deg.

4) Hinge moment and root bending moment are also predicted within 15%.

References

[1] Burkhalter, J. E., and Frank, H. M., "Grid Fin Aerodynamics for Missile Applications in Subsonic Flow," *Journal of Spacecraft and Rockets*, Vol. 33, No. 1, 1996, pp. 38–44.

[2] Burkhalter, J. E., Hartfield, R. J., and Leleux, T. M., "Nonlinear Aerodynamic Analysis of Grid Fin Configurations," *Journal of Aircraft*, Vol. 32, No. 3, 1995, pp. 547–554.

[3] Kretzschmar, R. W., and Burkhalter, J. E., "Aerodynamic Prediction Methodology for Grid Fins," *Proceedings of the NATO RTO Applied Vehicle Technology Panel Symposium on Missile Aerodynamics*, RTO-MP-5, NATO Research and Technology Organization, Cedex, France, Nov. 1998, pp. 11.1–11.11.

[4] Burkhalter, J. E., "Grid Fins for Missile Application in Supersonic Flow," *34th AIAA Aerospace Sciences Meeting & Exhibit*, AIAA Paper 1996-194, Jan. 1996.

[5] Theerthamalai, P., and Nagarathinam, M., "Aerodynamic Analysis of Grid Fin Configurations at Supersonic Flows," *Journal of Spacecraft and Rockets*, Vol. 43, No. 4, 2006, pp. 750–756.

[6] Khalid, M., Sun, Y., and Xu, H., "Computation of Flows Past Grid Fin Missiles," *Proceedings of the NATO RTO Applied Vehicle Technology Panel Symposium on Missile Aerodynamics*, RTO-MP-5, NATO Research and Technology Organization, Cedex, France, Nov. 1998, pp. 12.1–12.11.

[7] Lin, H., Huang, J. C., and Chieng, C.-C.,"Navier–Stokes Computations for Body/Cruciform Grid Fin Configuration," *Journal of Spacecraft and Rockets*, Vol. 40, No. 1, 2003, pp. 30–38.

[8] DeSpirito, J., Edge, H. L., Weinacht, P., Sahu, J., and Dinavahi, S. P. G., "CFD Analysis of Grid Fins for Maneuvering Missiles," *38th AIAA Aerospace Sciences Meeting & Exhibit*, AIAA Paper 2000-391, Jan. 2000.

[9] Chen, S., Khalid, M., Xu, H., and Lesage, F., "Comprehensive CFD Investigation of Grid Fins as Efficient Control Surface Devices," *38th AIAA Aerospace Sciences Meeting & Exhibit*, AIAA Paper 2000-987, Jan. 2000.

[10] Washington, W. D., Booth, P. F., and Miller, M. S., "Curvature and Leading Edge Sweep Back Effects on Grid Fin Aerodynamics," *AIAA Applied Aerodynamics Conference*, AIAA Paper 1993-3480, Aug. 1993.

[11] Miller, M. S., and Washington, W. D., "Experimental Investigation of Grid Fin Drag Reduction Techniques," *Proceedings of 12th Applied Aerodynamics Conference*, AIAA Paper 1994-1914, June 1994.

[12] Washington, W. D., and Miller, M. S., "Experimental Investigation of Grid Fin Aerodynamics: A Synopsis of Nine Wind Tunnel and Three Flight Tests," *Proceedings of the NATO RTO Applied Vehicle Technology Panel Symposium on Missile Aerodynamics*, RTO-MP-5, NATO Research and Technology Organization, Cedex, France, Nov. 1998, pp. 10.1–10.14.

[13] Mendenhall, M. R., and Nielsen, J. N., "Effect of Symmetrical Vortex Shedding on the Longitudinal Aerodynamic Characteristics of Wing-Body-Tail Combinations," NASA CR-2473, Jan. 1975.

[14] Mendenhall, M. R., Perkins, S. C., Jr., and Lesieutre, D. J., "Tactical Missile Aerodynamics: Prediction Methodology," *Progress in Astronautics and Aeronautics*, Vol. 142, 1992, Chap. 6.

[15] Horener, S. F., *Fluid-Dynamic Drag*, Hoerner Fluid Dynamics, Bakersfield, CA, 1993, Chap. 16.